

The Role of Target Signatures in Bird-Drone Classification

Atkinson, George; Jahangir, Mohammed; White, Daniel; Wayman, Joseph P. ; Baker, Chris; Sadler, Jon; Reynolds, Jim; Antoniou, Michail

DOI:

[10.1109/RadarConf2351548.2023.10149665](https://doi.org/10.1109/RadarConf2351548.2023.10149665)

License:

None: All rights reserved

Document Version

Peer reviewed version

Citation for published version (Harvard):

Atkinson, G, Jahangir, M, White, D, Wayman, JP, Baker, C, Sadler, J, Reynolds, J & Antoniou, M 2023, The Role of Target Signatures in Bird-Drone Classification. in *2023 IEEE Radar Conference (RadarConf23)*, 10149665, Proceedings of the IEEE Radar Conference, IEEE, 2023 IEEE Radar Conference, RadarConf23, San Antonio, United States, 1/05/23. <https://doi.org/10.1109/RadarConf2351548.2023.10149665>

[Link to publication on Research at Birmingham portal](#)

Publisher Rights Statement:

© 2023 IEEE. Personal use of this material is permitted. Permission from IEEE must be obtained for all other uses, in any current or future media, including reprinting/republishing this material for advertising or promotional purposes, creating new collective works, for resale or redistribution to servers or lists, or reuse of any copyrighted component of this work in other works.

General rights

Unless a licence is specified above, all rights (including copyright and moral rights) in this document are retained by the authors and/or the copyright holders. The express permission of the copyright holder must be obtained for any use of this material other than for purposes permitted by law.

- Users may freely distribute the URL that is used to identify this publication.
- Users may download and/or print one copy of the publication from the University of Birmingham research portal for the purpose of private study or non-commercial research.
- User may use extracts from the document in line with the concept of 'fair dealing' under the Copyright, Designs and Patents Act 1988 (?)
- Users may not further distribute the material nor use it for the purposes of commercial gain.

Where a licence is displayed above, please note the terms and conditions of the licence govern your use of this document.

When citing, please reference the published version.

Take down policy

While the University of Birmingham exercises care and attention in making items available there are rare occasions when an item has been uploaded in error or has been deemed to be commercially or otherwise sensitive.

If you believe that this is the case for this document, please contact UBIRA@lists.bham.ac.uk providing details and we will remove access to the work immediately and investigate.

The Role of Target Signatures in Bird-Drone Classification

George Atkinson
*Microwave Integrated
Systems Laboratory
(MISL)*
University of Birmingham
Birmingham, UK
g.m.atkinson@bham.ac.uk

Mohammed Jahangir
*Microwave Integrated
Systems Laboratory
(MISL)*
University of Birmingham
Birmingham, UK
m.jahangir@bham.ac.uk

Daniel White
*Microwave Integrated
Systems Laboratory
(MISL)*
University of Birmingham
Birmingham, UK
dxw636@bham.ac.uk

Joseph Wayman
*School of Geography,
Earth and Environmental
Sciences*
University of Birmingham
Birmingham, UK
j.wayman@bham.ac.uk

Chris Baker
*School of Engineering
University of Birmingham*
Birmingham, UK
c.j.baker.1@bham.ac.uk

Jon Sadler
*School of Geography,
Earth and Environmental
Sciences*
University of Birmingham
Birmingham, UK
j.p.sadler@bham.ac.uk

James S. Reynolds
*School of Biosciences
University of Birmingham*
Birmingham, UK
*The Army Ornithological
Society*
c/o Price Consort Library
Aldershot, UK
j.reynolds.2@bham.ac.uk

Michail Antoniou
*Microwave Integrated
Systems Laboratory
(MISL)*
University of Birmingham
Birmingham, UK
m.antoniou@bham.ac.uk

Abstract— Mapping and characterising low to medium airspace in an urban setting using radar presents significant challenges, especially for low observable targets such as drones and birds. This paper presents some examples of micro-Doppler signatures which make up part of a larger dataset of control drone, control bird, and opportune bird signatures measured with a pair of L-band staring radars installed at an urban location at the University of Birmingham. The results of multiple measurements over a two-year period are used to facilitate the classification of birds and drones, and the results of a machine learning classifier on the collected data is shown.

Keywords—L-Band, staring radar, urban surveillance

I. INTRODUCTION

With the increasing prevalence of drones in low altitude urban airspace, the capability to map this airspace using wide-area surveillance radar requires the reliable and accurate detection, tracking, and identification of drones, as well as the ability to distinguish these drones from confuser targets such as birds. Additionally, the identification of bird targets is important when considering, for example, the security and safety of a runway, as well as for monitoring the activity of birds in an urban environment in aeroecology research.

The detection, tracking, and identifying small targets in low-altitude airspace of an urban environment poses a significant challenge due to the dense clutter of such an environment. Several strategies for classifying drones using radar systems have been proposed, using both kinematic features and micro-Doppler features, utilising both decision tree-based classification as well as deep learning [1]–[3]. For classification using deep learning methods, Convolutional Neural Networks (CNNs) provide some of the best results when a target’s spectra contains micro-Doppler components induced by the rotating parts of a drone. While some research has shown classification without the need to label non-drone targets explicitly [4], other research has proposed methods for labelling opportune targets [5] allowing supervised learning techniques to benefit from large quantities of labelled drone and bird target data [6]. At the University of Birmingham (UoB), two L-band staring radars have been installed capable

of detecting and tracking small and low radar cross section (RCS) targets. The staring radar offers an all-weather solution to track targets reliably and accurately in real-time with minimal false tracks, and additionally provides the high sensitivity and high Doppler resolution necessary to track low RCS targets which fly at low altitudes and low velocities [7], [8]. The testbed facility enables the collection of vast amounts of data from both opportune targets, as well as from a diverse set of controlled flights of drone and bird targets in a variety of urban areas.

This paper presents some of the micro-Doppler signatures of control drone and bird targets as well as the results of a CNN classifier trained and tested on spectrogram images, that is able to distinguish between birds and drones with a high accuracy. Section II provides an overview of the UoB staring radar facility, section III details the measurement campaigns conducted to collect a multitude of drone and bird signatures, section IV presents some examples of results from this measurement campaign focusing on the characteristics of the Doppler spectrograms for each target type, section V presents some classification results using a CNN classifier utilising the dataset collected, and, finally, section VI presents the conclusions and future work.

II. INFRASTRUCTURE SETUP

The UoB is developing a dedicated facility of networked staring radars to capture, from the urban environment, realistic clutter over extended periods of time [9]. The facility consists of two L-band multiple receive beam 3-D staring radar systems installed on the rooftops of buildings on the UoB Edgbaston campus, approximately 4 kilometers away from Birmingham city centre. The first radar is located atop the 6-story Gisbert Kapp building at a height of 108 m above sea level (ASL). The second radar is located on the roof of the European Research Institute (ERI) building on the Edgbaston campus, approximately 180 m from the first radar, and at a height of 90 m ASL. Each radar is a prototype commercial-off-the-shelf system that are designed for the detection of small, low-altitude, low-RCS objects, such as micro-Unmanned Aerial Vehicles (UAVs) and birds. Operating at L-

band and using a broad beam on transmit and 2-D array on receive that are digitised at element level, the radar can provide multiple simultaneous digital beams over its field of regard that spans 90 degrees in azimuth and 60 degrees in elevation. It has an instrumented range of up to 10 km [5-6]. The radar has a low bandwidth <2 MHz but uses a pulse waveform with a high PRF (~ 8 kHz) and is therefore able to achieve long integration and a high update rate on targets.

Baseband I/Q data for a specified range gates can be saved to disk for every pulse for all receiver channels. Doppler processing and beam forming are performed in software. The radar system also has an on-board real-time processor that performs standard detection on the beam-formed range-Doppler data and, following a tracking and classification stage, outputs tracker data that is updated every frame for all active tracks. The frame update rate is software configurable but typically is about 0.25 seconds. The tracker output has an associated track ID and target classification label that assigns broad class labels such as drone, birds, ground targets, unknown etc. Both the raw data and the processed tracker output are available for off-line analysis and processing. The radar facility is capable of continuous operation although the duration for which raw data can be saved is limited by the available storage space. Each radar is capable of operating monostatically or as part of a network. All results reported in this paper are from monostatic configurations of either of the two radars.

III. MEASUREMENTS CAMPAIGN

A. Control Drone Measurements

To obtain a diverse dataset of target signatures, multiple different types of drone were flown at a variety of distances, heights, and speeds. Figure 1 shows some of the rotary wing drones used for field trials, a DJI Inspire 2 (I3-D), a DJI Mavic Mini 2 (M2-D), and a DJI Matrice 300 (MT-D). The GPS position of each drone is acquired from the log files recorded by the drone, which for some of the drone models also includes the rotational speeds of each rotor, which can be used to generate realistic simulated micro-Doppler signatures for synthetic targets [10].



Figure 1 – (a) DJI Inspire 2 (I3-D), (b) DJI Mavic Mini 2 (M2-D), (c) DJI Matrice 300 (MT-D)



Figure 2 – GPS tracks from one of the drone trials, from Google Earth

The larger drones such as the MT-D and I3-D were flown using pre-programmed waypoints which allowed the drones to repeat a predetermined flight path at a number of different heights. The smaller drones could not be flown using waypoints and so they were flown manually by an operator on a straight path between the same predetermined waypoints for the larger drones. Figure 2 shows the GPS plot from one of

the drone trials. Over 10 hours of drone flight data has been collected using this methodology.

B. Control Bird Measurements in a Rural Environment

Measurements of control birds require that birds are tagged with a GPS device to record accurate position, and that they fly within the field of view of the radar. For this reason, control bird measurements require the use of captive birds flown by trained professional handlers [11]. A control trial at a rural location with raptors was conducted in collaboration with the International Centre for Birds of Prey (ICBP), in which four birds were flown in the field of view of an L-band staring radar installed at Cranfield Airport. The four birds used for the trial were a Saker Falcon (*Falco cherrug*) \times Gyrfalcon (*Falco rusticolus*) hybrid (hereafter referred to as the ‘hybrid falcon’), a Gyrfalcon, a Yellow-billed Kite (*Milvus aegyptius*), and a Black-chested Buzzard-eagle (*Geranoaetus melanoleucus*). Each bird was tagged with a Microsensory GPS tracking device which was capable of real-time positioning of the bird, with the use of a handheld receiver, as well as being able to store the GPS data for later retrieval. The birds were released approximately 1.75 km from the staring radar in an open area with direct line of sight. The hybrid falcon and Gyrfalcon were trained to chase a small, fixed-wing UAV designed to look like a bird, known as the RoboCrow. This drone was piloted by one of the handlers from the ICBP and flown in a circular trajectory. The Yellow-billed Kite was flown from one handler to another close to the ground. The Black-chested Buzzard-eagle, when released, rose up to approximately 200 m above the ground and flew in a tight circular pattern while being carried towards the radar by the prevailing wind.



Figure 3 – (a) Black-chested Buzzard-eagle equipped with a Microsensory GPS tracking device, and (b) GPS track generated during flight shown in Google Earth

Figure 3a is a photograph of the Black-chested Buzzard-eagle, the largest of the birds flown during the trial and Figure 3b shows the GPS track of the bird, superimposed onto an aerial image of the target location, with the radar field of view also shown. The circling behaviour exhibited by the bird manifests as a spiral pattern in the GPS track due to the overall motion towards the radar as a result of the wind direction on the day and at the altitude the bird flew. From this study, 18 minutes of truthed bird flight data was collected.

C. Control Bird Measurements in an Urban Environment

For control bird measurements in an urban environment, a field trial was conducted in which homing pigeons (*Columbia livia domestica*) were equipped with PathTrack GPS tracking tags and released within the field of view of an L-band staring radar. When released, homing pigeons first fly in a sweeping circle over the immediate area before flying in the direction of their home loft in the north-east of the city. The birds were released from Queen's Park, just over 2.5 km from the radar. Each bird wore a custom-made harness designed to hold a tracking tag (Fig. 4), which provided high-accuracy and high-

update positional data for the bird. The GPS tag was activated prior to the release of a pigeon and recorded its position onto an internal memory card at a rate of 5 Hz. Each tag can only record up to an hour of high-rate data due to the limits of the internal memory.



Figure 4 – Homing pigeon with a harness carrying a PathTrack GPS tag

Once the birds had returned to the loft, the data was downloaded from each of the tags. For the period of time the birds flew in the field of view of the radar, typically the first few minutes of flight, the positional GPS data were in all cases captured and recorded. Figure 5 shows an aerial image showing locations of the release site and the loft as well as the location and field of view of the staring radar. The image shows different coloured tracks depicting the flight paths of the birds which were released individually.

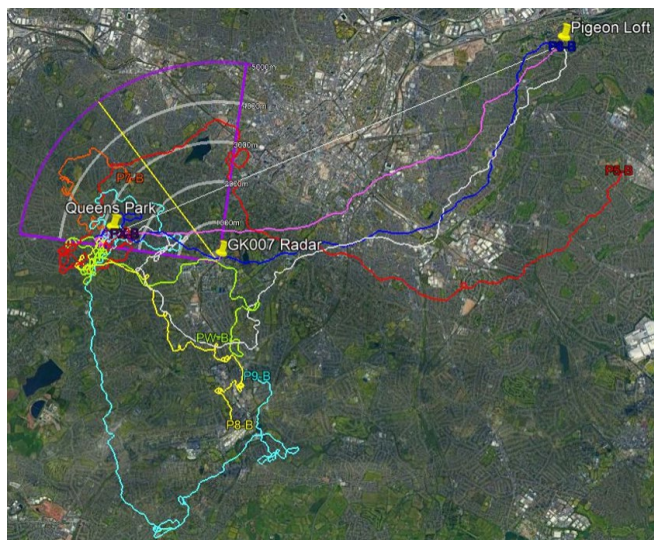


Figure 5 - Image showing the GPS tracks of multiple racing pigeons superposed on an aerial image of the scene with the radar coverage shown

D. Opportune Bird Measurements

By far the largest dataset collected to date is that of opportune bird targets, including raw data of opportune birds when recording for control drone and bird trials. Raw data for over 10 hours of opportune flights has been recorded. However, without any truthing, the data are unlabelled and therefore not ideal for classification using supervised learning algorithms.

A technique for truthing opportune birds by matching field observation to the radar tracker output has been developed. The transect method involves an observer recording the traverse(s) of a bird across a virtual line between the observer and a fixed point, usually a landmark

such as a tall building. The time, crossing direction, approximate distance, and approximate height, are recorded by the observer when a bird crosses this virtual line, known as a ‘transect line’. Comparing these crossing observations to the track number (referred to as ‘track ID’) which cross the transect line at approximately the same time and in the same direction, individual observations can be matched to track IDs, leading to a labelled set of opportune bird tracks. To date, twelve transect trials have been performed at different locations within the field of view of the test bed facility. For some of these trials, raw radar data were recorded, allowing us to produce a species-labelled set of opportune bird spectrograms.

IV. RESULTS

In order to investigate the micro-Doppler signatures of drones and birds, the raw data were processed into spectrograms of the targets, which showed the Doppler profile per Coherent Processing Interval (CPI) as a function of time for a target at a particular range and beam direction. To generate a target spectrogram, firstly all beam directions for each CPI were processed into range-Doppler plots. The GPS positional data of the drone or bird were then used to determine the target range and beam direction, and the Doppler profile for each CPI was then concatenated to form the spectrogram. In the resulting spectrogram images, static clutter appeared as a bright line through the centre of the image, as this represented reflectors with zero Doppler at all time points. The body of the drone or bird, when visible above the noise floor, appeared as a line offset from the center with non-zero Doppler. Since the Doppler axis represents the radial velocity of the target, the body return may cross through the zero-Doppler clutter line when the component of velocity in the radial direction changes direction such as when the target is moving in a circular trajectory. Sub-components of a target object which oscillate at higher frequencies, such as the rotational motion of drone propellers or the flapping motion of bird wings, can result in detectable micro-Doppler components in the spectrograms. These micro-Doppler signatures can be used to help to discriminate between targets such as drones and birds. Furthermore, for drones there is a strong correlation between the micro-Doppler signature and the physical parameters relating to the rotors and have shown to enable estimation of the blade length and rotation rate of the propellers that in turn can help to identify sub-categories of a drone class, such as the approximate size of the drone [12].

A. Drone Micro-Doppler Results

The drone spectrograms shown in Figure 6 in this section are from target measurements that were conducted at the same range of <2km. Figure 6a shows the spectrogram for MT-D showing strong micro-Doppler Helicopter Rotor Modulation (HERM) lines that are due to the drone’s rotor motion [10], which takes the appearance of spectral lines in this case where the blade’s rotational rate is greater than the integration length of the CPI. Note that between timestep 250 and 350 the micro-Doppler is observed to split into four components, showing the individual contributions from each of the four rotors of the quadcopter drone. Figure 6b shows the spectrogram for I3-D flying the same trajectory as that of MT-D. Again, the rotating propeller blades from the four rotors of this drone produced highly visible micro-Doppler lines throughout the measurement time period. In contrast to

the micro-Doppler observable in the spectrogram for MT-D, the micro-Doppler signature appeared weaker and less uniform, and the sideband splitting due to the individuality of rotor speeds is of a different character. Both drones present strong micro-Doppler at all times, with sideband-to-body ratio existing at approximately -20dB. Figure 6c shows the spectrogram for the smaller M2-D drone. The micro-Doppler appears very different in comparison to the other two drones, due to the smaller rotor blades of the M2-D drone that reflect insufficient energy relative to the noise floor to appear in the spectrogram. Also, as this drone was flown manually (unlike I3-D and MT-D that were flown using pre-programmed waypoints) the body return of the drone was more irregular. All the subtle differences in the drone body and micro-Doppler signature characteristics can aid with target classification.

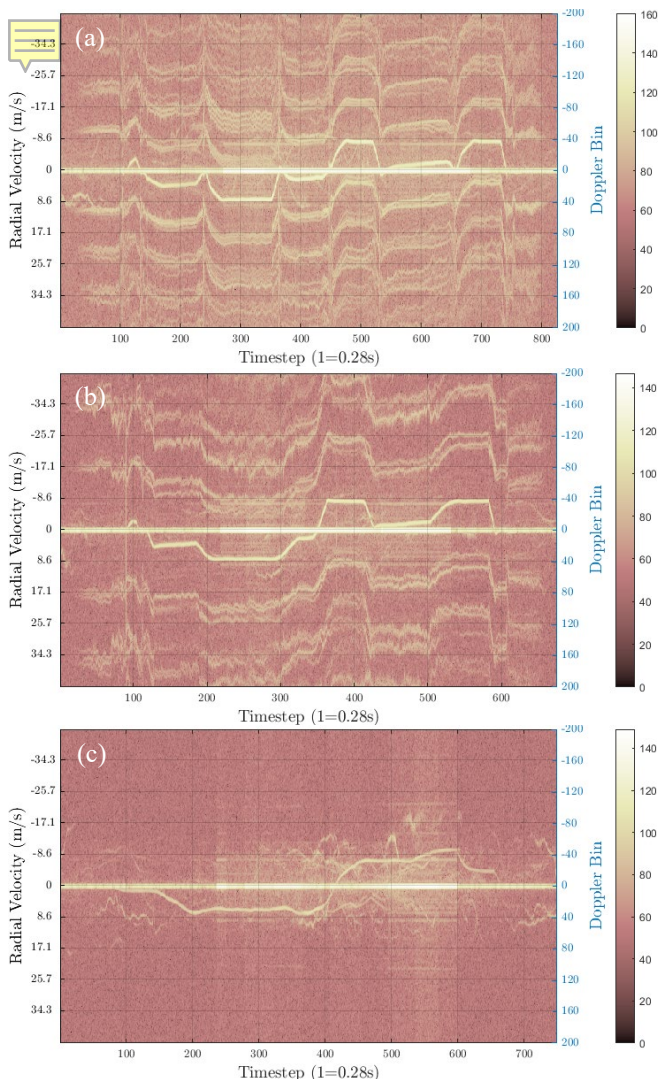


Figure 6 – Spectrograms of the (a) DJI Matrice 300 (MT-D), (b) DJI Inspire 2 (I3-D), and (c) DJI Mavic Mini 2 (M2-D) drone targets

B. Control Bird Micro-Doppler Results

Figure 7a shows the spectrogram from the Black-chested Buzzard-eagle that was circling during its flight and the resulting body return can be seen to oscillate through zero Doppler line for the majority of the measurement. The body return itself is very narrow and weaker than those of the drone targets shown previously. Note the absence of any strong micro-Doppler in the spectrogram and visually it appears

highly differentiated from the drone spectra shown in Figure 6a and b. Figure 7b shows the spectrogram for one of the homing pigeons from the control pigeon trial. However, unlike the Black-chested Buzzard-eagle, the spectrogram contained what appears to be faint sideband lines but with a closer spacing between them. This was most evident between timesteps 300 and 500 in Figure 7b. Although the precise origin of these micro-Doppler lines is unknown, one possibility is the oscillating motion of the wings of the bird as they flap. When the pigeons flew from the release site to the loft they were observed flapping their wings rapidly while in visible range. This was in contrast to the larger birds of prey such as Black-chested Buzzard-eagle that tended to glide when possible, flapping its wings less frequently than the pigeons. Given the very different appearances of the bird spectrograms from those of drones when HERM lines are present, it was envisaged that a classification algorithm would be able to discriminate between drones and birds on the basis of their spectra.

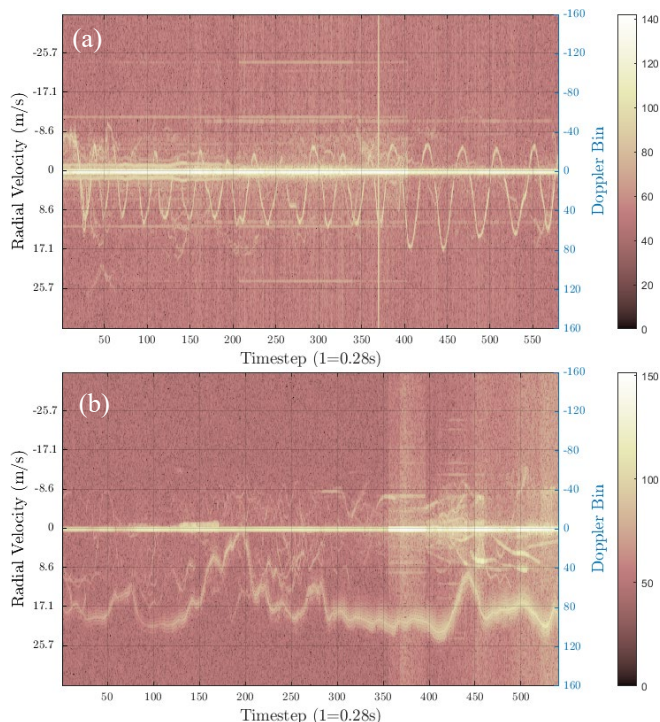


Figure 7 – Spectrograms of the (a) Black-chested Buzzard-eagle, and (b) homing pigeon bird targets

C. Opportune Bird Micro-Doppler Results

For the spectrograms of opportune birds, recorded in the urban environment around UoB, the Doppler characteristics varied markedly but in general there was a lack of micro-Doppler sidebands that were typical of those observed for larger drones. However, the characteristics of the body return observable in the spectrograms for the opportune birds showed some distinguishable properties. For example, Figure 8a shows a spectrogram from an opportune bird target in which the body Doppler was narrow, while Figure 8b shows a spectrogram of another opportune bird in which it was much broader. Figure 8c shows a spectrogram of an opportune bird displaying some of the same micro-Doppler signature characteristics as observed in Figure 7b, and thus was assumed to also be a pigeon.

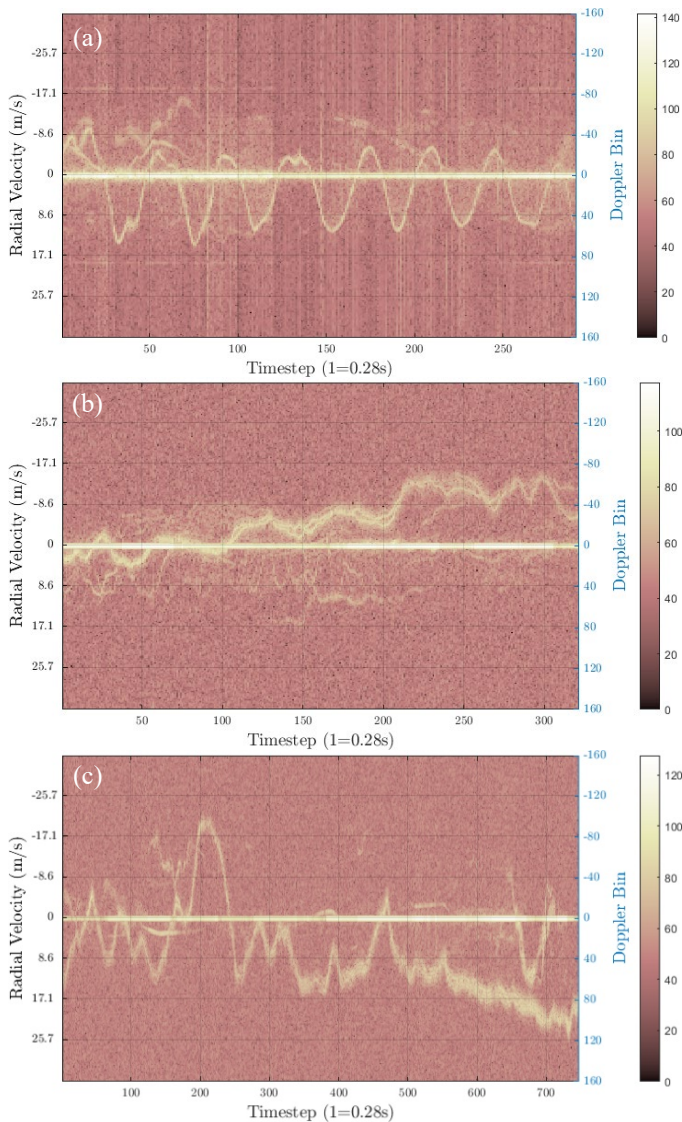


Figure 8 – Spectrograms of opportune bird targets with Doppler signatures that are (a) narrow, (b) broad, and (c) appear similar to those of a pigeon as shown in Figure 7b.

Due to the resolution of the staring radar, it is possible to record multiple birds within a resolution cell. During trials, flocking behaviour of birds has been observed and recorded by the radar as an opportune measurement. The spectral characteristics of a group or flock of birds can be observed in Figure 9 that depicts two spectrograms, each with multiple spectral lines indicative of a collection of multiple bird targets in close proximity to each other and demonstrating similar flight patterns. In addition, Figure 9b shows the spectrogram from a dense cluster of birds, where individual spectral lines can no longer be distinguished at all points in time, but the spectra of the return signature is markedly wider than that of an individual bird target return. Given the difference in the appearance of the spectra of flocks from those of individual birds or drones, there is potential to derive classification approaches for flock detection. We report these results captured by an L-band staring radar. At other operational frequencies the scattering nature of flocks may be different, and the detail observed in bird micro-Doppler may be greater [13].

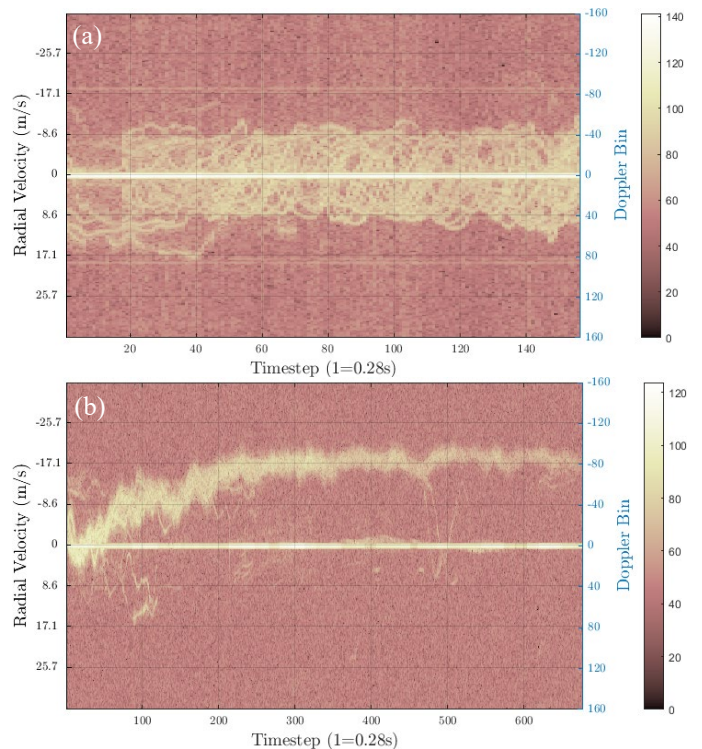


Figure 9 – Spectrogram of a flock of opportune bird targets

V. DRONE-BIRD CLASSIFICATION

Recently published results using CNNs to classify drones and birds have demonstrated that they work well for high Signal to Noise Ratio (SNR) data in which distinguishing micro-Doppler features are present [14]. With the large dataset of drone and bird spectrograms from the UoB testbed, a CNN classifier was trained to understand performance within a realistic urban setting. The classifier used in this case was a pretrained neural network called Alexnet, which was then retrained in the last three layers to classify full colour spectrograms input as images. The classifier was configured to detect only drones and birds, and all drone spectra were obtained from well labelled control trials and the bulk of bird spectra were obtained from opportune targets where the true label was unknown.

TABLE 1. TARGET QUANTITIES USED IN CNN TRAIN AND TEST SETS

Set (#Images)	Class (#Images)	Target	#Flights	#Images
Train (7,256)	Bird (3,625)	Control	-	-
		Opportune	321	3625
	Drone (3,631)	I3-D	46	1444
		MT-D	29	1058
		M2-D	40	1129
Test (3,632)	Bird (1,818)	Control	3	137
		Opportune	143	1681
	Drone (1,814)	I3-D	19	612
		MT-D	19	671
		M2-D	19	531

Table 1 shows the quantities of the train and test subsets. The subsets were randomly constructed, ensuring that images from a given flight were not mixed across different sets. Each

image corresponded to five seconds of dwell time on the target. Figure 10 shows the results of the CNN classification as a confusion matrix. The percentage of correctly classified spectrograms for birds and drones was 90.1% and 90.0%, respectively.

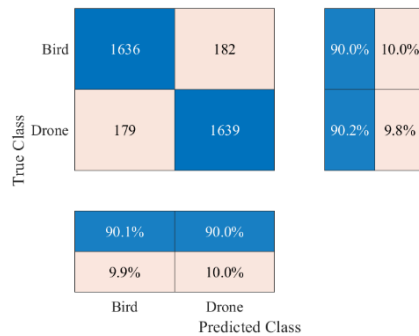


Figure 10 – Confusion matrix of a CNN classifier between birds and drones

While the CNN classifier provided a good accuracy for distinguishing birds and drones, the classifier works by identifying spatial features in spectrograms, such as the shape and distribution of micro-Doppler lines. In addition to these geometric features, it may be possible to categorize targets based on other features which can be derived from the spectrograms, such as SNR of a target, as well as features extracted from the trajectory information of a target, which can be determined from the output of the tracker and does not require raw data or spectrograms to be generated.

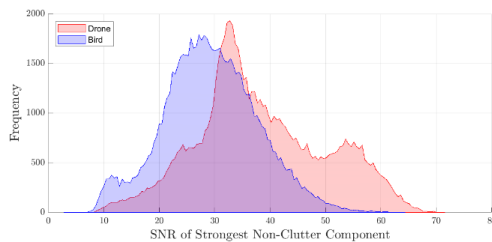


Figure 11 - Histogram of the SNR of the strongest non-clutter component of each target's spectrogram.

Figure 11 shows a histogram of the measured SNR for a multitude of bird and drone targets. As can be seen, there was a large overlap of SNR values for drones and birds. However, there were non-overlapping regions in which the lower SNR can be attributed to birds, while the higher SNR values can be attributed to drones.

VI. CONCLUSIONS AND FUTURE WORK

This paper describes the measurement campaign conducted with the UoB staring radar facility and showcases some of the characteristics of the Doppler signatures of control drone, control bird, and opportune bird targets. The empirical results highlighted many of the differences (and similarities) between the bird and drone signatures which present real challenges to the development of classifiers designed to distinguish between drones and birds. Using the large dataset of labelled measurements collected with the UoB staring radar testbed, a CNN classifier was performed and gave a classification accuracy of 90.1% on a test set of 3,632 images. For further classification, it is not yet known to what extent the classifiers can distinguish between individual and groups of birds, and to what extent flocks of birds affect the broader classification of drones versus birds. Using the

dataset collected, it is becoming possible to investigate whether there is a need to separate measurements which contain flock behaviour from those of individual targets, and to test the effectiveness of the classifier in distinguishing between individual bird species and drone models.

ACKNOWLEDGMENTS

The work was funded by the UK National Quantum Technology Hub in Sensing and Timing (EP/T001046/1) and the EPSRC MEFA (EP/T011068/1) projects. The authors are grateful to Aveillant Ltd for helping with installing the radar and their ongoing engagement with the research work supported by the testbed.

REFERENCES

- [1] D. A. Brooks, O. Schwander, F. Barbaresco, J.-Y. Schneider, and M. Cord, 'Complex-valued neural networks for fully-temporal micro-Doppler classification', in *2019 20th International Radar Symposium (IRS)*, 2019, pp. 1–10. doi: 10.23919/IRS.2019.8768161.
- [2] H. Dale, C. Baker, M. Antoniou, and M. Jahangir, 'An Initial Investigation into Using Convolutional Neural Networks for Classification of Drones', in *2020 IEEE International Radar Conference (RADAR)*, 2020, pp. 618–623. doi: 10.1109/RADAR42522.2020.9114745.
- [3] C. Bennett, M. Jahangir, F. Fioranelli, B. I. Ahmad, and J. L. Kerneć, 'Use of Symmetrical Peak Extraction in Drone Micro-Doppler Classification for Staring Radar', in *2020 IEEE Radar Conference (RadarConf20)*, 2020, pp. 1–6. doi: 10.1109/RadarConf2043947.2020.9266702.
- [4] M. Jahangir, B. I. Ahmad, and C. J. Baker, 'The Application of Performance Metrics to Staring Radar for Drone Surveillance', in *2020 17th European Radar Conference (EuRAD)*, 2021, pp. 382–385. doi: 10.1109/EuRAD48048.2021.00104.
- [5] J. Sim, M. Jahangir, F. Fioranelli, C. J. Baker, and H. Dale, 'Effective Ground-Truthing of Supervised Machine Learning for Drone Classification', in *2019 International Radar Conference (RADAR)*, Sep. 2019, pp. 1–5. doi: 10.1109/RADAR41533.2019.171322.
- [6] H. Dale, M. Jahangir, C. J. Baker, M. Antoniou, S. Harman, and B. I. Ahmad, 'Convolutional Neural Networks for Robust Classification of Drones', in *2022 IEEE Radar Conference (RadarConf22)*, 2022, pp. 1–6. doi: 10.1109/RadarConf2248738.2022.9764172.
- [7] M. Jahangir, C. J. Baker, and G. A. Oswald, 'Doppler characteristics of micro-drones with L-Band multibeam staring radar', in *2017 IEEE Radar Conference (RadarConf)*, May 2017, pp. 1052–1057. doi: 10.1109/RADAR.2017.7944360.
- [8] A. Coluccia, G. Parisi, and A. Fascista, 'Detection and Classification of Multirotor Drones in Radar Sensor Networks: A Review', *Sensors*, vol. 20, no. 15, 2020, doi: 10.3390/s20154172.
- [9] M. Jahangir et al., "Networked staring radar testbed for urban surveillance: status and preliminary results," International Conference on Radar Systems (RADAR 2022), Hybrid Conference, Edinburgh, UK, 2022, pp. 471–476, doi: 10.1049/icp.2022.2363.
- [10] D. White et al., "Multi-rotor Drone Micro-Doppler Simulation Incorporating Genuine Motor Speeds and Validation with L-band Staring Radar," 2022 IEEE Radar Conference (RadarConf22), 2022, pp. 1–6, doi: 10.1109/RadarConf2248738.2022.9764352.
- [11] M. Jahangir, G. M. Atkinson, M. Antoniou, C. J. Baker, J. P. Sadler, and S. J. Reynolds, 'Measurements of birds and drones with L-Band staring radar', in *2021 21st International Radar Symposium (IRS)*, 2021, pp. 1–10. doi: 10.23919/IRS51887.2021.9466224.
- [12] X. Ren, M. Jahangir, D. White, G. M. Atkinson, C. J. Baker and M. Antoniou, "Estimating physical parameters from multi-rotor drone spectrograms," International Conference on Radar Systems (RADAR 2022), Hybrid Conference, Edinburgh, UK, 2022, pp. 20–25, doi: 10.1049/icp.2022.2285.
- [13] H. Dale, C. Baker, M. Antoniou, M. Jahangir, G. Atkinson, and S. Harman, 'SNR-dependent drone classification using convolutional neural networks', *IET Radar Sonar Navig.*, vol. 16, no. 1, pp. 22–33, Jan. 2022, doi: 10.1049/rsn2.12161.
- [14] S. Rahman & D. A. Robertson, 'Radar micro-Doppler signatures of drones and birds at K-band and W-band', *Scientific Reports*, vol. 8, 17396, 2018. doi:10.1038/s41598-018-35880-9